Temporal summation in a neuromimetic micropillar laser

F Selmi, R Braive, G Beaudoin, I Sagnes, R Kuszelewicz, Sylvain Barbay

Temporal summation in a neuromimetic micropillar laser

F. Selmi,[1] R. Braive,[1] G. Beaudoin,[1] I. Sagnes,[1] R. Kuszelewicz,[2] and S. Barbay[1,*]

[1] *Laboratoire de Photonique et de Nanostructures, LPN-CNRS UPR20, Route de Nozay, 91460 Marcoussis, France*

[2] *Neurophotonics laboratory, Université Paris Descartes, 12 rue de l'École de Médecine, 75270 Paris Cedex 06, France*

Neuromimetic systems are systems mimicking the functionalities or architecture of biological neurons and may present an alternative path for efficient computing and information processing. We demonstrate here experimentally temporal summation in a neuromimetic micropillar laser with integrated saturable absorber. Temporal summation is the property of neurons to integrate delayed input stimuli and to respond by an all-or-none kind of response if the inputs arrive in a sufficiently small time window. Our system alone may act as a fast optical coincidence detector and paves the way to fast photonic spike processing networks.

Neuromimetic photonic systems are optical systems that mimic the functionalities or the architecture of biological neurons, and can represent an alternative path for computing and processing information very efficiently both in terms of energy, speed, and robustness versus noise [1, 2].

From a functional and basic point of view, a biological neuron can be thought of as a system than can integrate information from various stimuli, and respond in an all-or-none fashion if the integrated input stimuli exceed a certain threshold [3]. This latter property is called excitability and has been experimentally demonstrated already in many nonlinear semiconductor optical systems, like active semiconductor cavities with feedback [4, 5], with optical injection [6–10] or with saturable absorber [11, 12]. The former property is called temporal summation. Temporal summation refers to the ability of the system to integrate different, potentially delayed, presynaptic stimuli and to emit a spike if the integration of the inputs exceeds the excitable threshold. Since in that case the system acts as an integrator, it has a time constant and the summation only takes place if the presynaptic stimuli arrive within in a given time window. While most of the cortical neurons are integrators [13], note that there also exists so called resonator neurons for which summation rules depend more on the phase of the input stimuli with respect to their subthreshold oscillation frequency [13, 14].

In optical systems, the response is in the form of an intensity spike with a characteristic shape and can be well under the nanosecond timescale [11, 15]. Following the demonstration of excitability in a planar semiconductor laser with integrated saturable absorber [11], it has been suggested [16] that this kind of system could act as a leaky integrate-and-fire neuron, a model of neuron widespread in neuroscience [17] and optically implemented with telecom components in [18].

The excitable response of micropillar lasers with integrated saturable absorber has been investigated in [12] demonstrating the absolute and relative refractory periods, in complete analogy to biological systems. In this Letter we investigate the response of a micropillar laser with integrated saturable absorber to sub-threshold stimuli and show that the system can integrate the stimuli and emit an excitable spike if the stimuli are close enough in time. This demonstrates temporal summation in this system and its ability to act as a fast optical coincidence detector [3, 19], a property usable for optical pattern recognition tasks. This property is also at the base of some neurocomputational models for e.g. sound localization in the barn owl auditory system [20]. It is also of paramount importance to fabricate optical neuromimetic circuits by e.g. coupling several micropillar units since, together with excitability, it demonstrates a fast and compact leaky integrate-and-fire optical neuron.

The experiment consists of a micropillar laser with integrated saturable absorber of original design described in [12, 21]. The micropillar is optically pumped by a laser diode array emitting around 800nm and emits light close to cavity resonance designed at 980nm. The active medium consists of two InGaAs/AlGaAs quantum wells while the saturable absorber medium has only one quantum well. Optical perturbations are sent to the system thanks to a Ti:Sa model-locked laser emitting $\sim$ 80ps duration pulses with a 80MHz repetition rate (see Figure 1). The rate can be down-sampled thanks to a pulse picker. A tunable delay line is inserted in the perturbation path allowing consecutive perturbations with a delay of several hundreds of picoseconds to several nanoseconds. The pump and perturbation beams are coupled into the micropillar thanks to a dichroic mirror and a microscope objective. Two fast avalanche photodetectors (APD_1 and APD_2) with 10GHz and 4GHz bandwidth respectively record the input pulses and the response from the micropillar. The signals are analyzed with a 6GHz oscilloscope.

The micropillar is driven in the excitable regime, 9% below the self-pulsing threshold, thus no laser light is emitted. Two consecutive sub-threshold perturbations are sent onto the micropillar at 797.5nm, close to the pump wavelength, with a variable delay δ. The first and second perturbation are set to 74% and 80% of the ex-

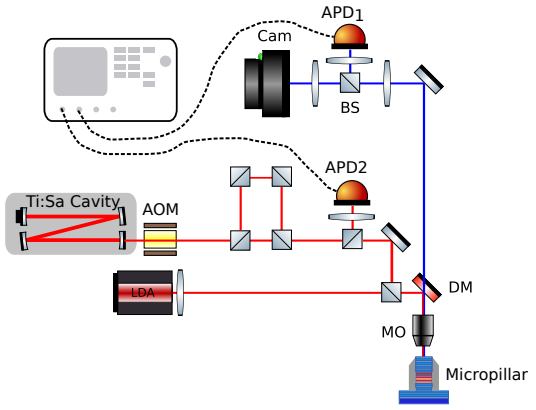

Figure 1. Experimental setup: LDA, laser diode array; DM, dichroic mirror; BS, beamsplitter; MO, microscope objective (63×, NA=0,85). Ti:Sa, mode-locked laser (80ps pulse duration); AOM, pulse picker; $APD_{1,2}$, avalanche photodiodes; Cam, CMOS camera.

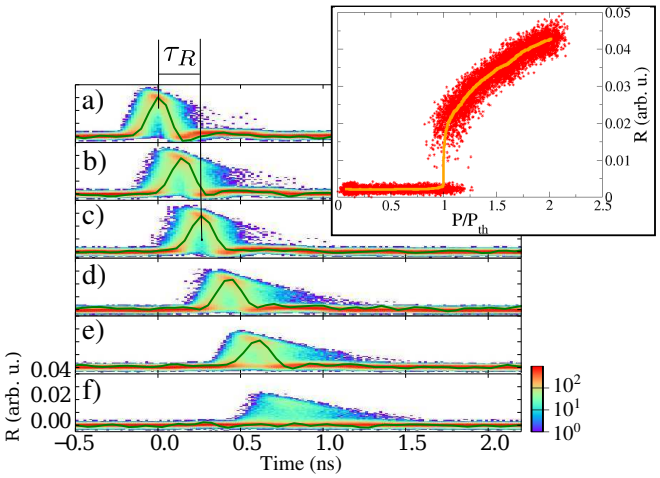

Figure 2. Experimental traces of the system's response to two incoming, sub-threshold perturbations for different perturbation delays δ : a) 210, b) 320, c) 420, d) 520, e) 610 and f) 700ps. The plots show the statistical density of points (in log scale) for 10000 different realizations. On the plots a typical response pulse is shown in green. Inset : excitable response to a single perturbation. Red stars are the detected response maxima. Orange is a plot of the median in a sliding window with 500 points.

citable threshold so that none of each perturbation is able by itself alone to trigger an excitable response. Since noise is present in the system (either internal, spontaneous emission noise or external noise sources such as pump noise or noise in the perturbation amplitude), we record the response of the system after sending 10000 identical perturbations. The results are shown on Fig.2. For a large perturbation delay (δ = 700ps, Fig.2f), the perturbations rarely adds-up to trigger an excitable response while for shorter ones, a clear, large amplitude response R is visible. This means that the system integrates the perturbations which produces an above-threshold stimulus able to trigger a large, excitable response. Note that the excitable response, when present, has always the shape depicted on Fig.2a) when a single event is plotted (green curve). The average response has a dispersion in time because of the dynamical delay induced by the noise, which can be mostly attributed to pump and perturbation noise. In order to quantify the response we plot in Fig.4a the median of the response amplitude R versus delay δ. A clear transition is visible in the amplitude : for delays below 610ps the perturbations trigger an excitable response and are thus temporally summed. For larger delays the summation does not occur anymore. This behavior is in stark contrast to the case of a gain-switched laser that would respond linearly. The transition depends on the excitable threshold value and thus on the bias pump [12], and on the amplitude of the incoming perturbations. Summation also occurs for a resonant perturbation at the cavity resonance close to 980nm, as can be seen on Fig.3. In that case, the excitation wavelength is λ = 980.471nm. The bias pump is set to 90% of the self-pulsing threshold in the excitable regime, as can be seen in the inset. The two perturbations are set 44% and 66% of the excitability threshold for the direct and delayed pulses respectively. They are clearly visible in the recorded traces and are marked by arrows. Temporal summation occurs for short delays (a), 220ps and to a lesser extent b) 350ps) and is absent for the other delays (c–e) 450, 540 and 630ps). Contrarily to the incoherent excitation case, the excitable curve in inset shows a marked plateau for stimuli above the excitable threshold. This behavior is important in view of cascading several excitable units. The fact that temporal summation is possible for incoherent (perturbation on the gain carrier density) and "coherent" (perturbation on intensity at cavity resonance) adds some flexibility to the system and has no counterpart in biological systems.

Note also that there is a delay of nonlinear origin in the response that depends on the summed perturbations (Fig.4a). This mechanism is interesting from a neuromimetic point of view since it provides a natural time-coding mechanism for the amplitudes : for a large input the delay is short, while it is long for a small (supra-threshold) summed input.

The experimental results are compared to numerical simulations of the Yamada model with spontaneous emission [11, 22]. This model reads:

$$\dot{I} = (G - Q - 1)I + \beta(G + \eta)^2 \quad (1)$$

$$\dot{G} = \gamma_g(\mu - G(1 + I)) \quad (2)$$

$$\dot{Q} = \gamma_{as}(\gamma - Q(1 + sI)) \quad (3)$$

. The dynamical variables are the intracavity intensity I, the gain G and the absorption Q. Recombination rates of carriers in the gain and saturable absorber sections are respectively γ_g and γ_{as}. Other parameters are s the

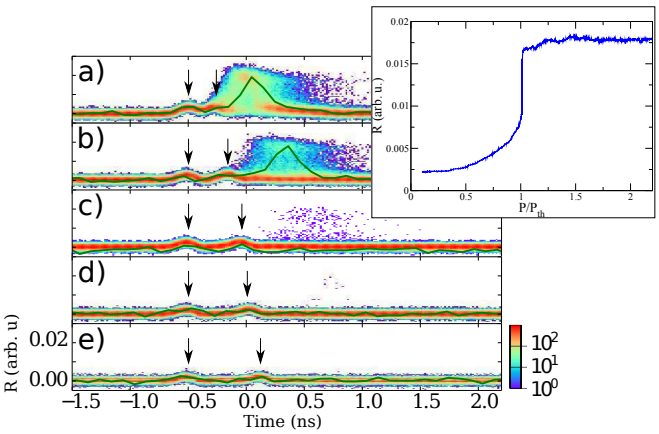

Figure 3. Coherent temporal summation with input perturbation wavelength $\lambda = 980.471$nm. The bias pumping is set to 90% of the self-pulsing threshold. The input stimuli are set to 44% and 66% of the excitability threshold for the direct and delayed pulses respectively. The plots show the statistical density of points (in log scale) for 10000 different realizations of the input perturbations with delays (a–e) : 220ps, 350ps, 450ps, 540ps and 630ps. On the plots, a typical response pulse is shown in green. The intensity perturbations are indicated by arrows. In inset : excitable response to a single perturbation median-averaged over 500 points.

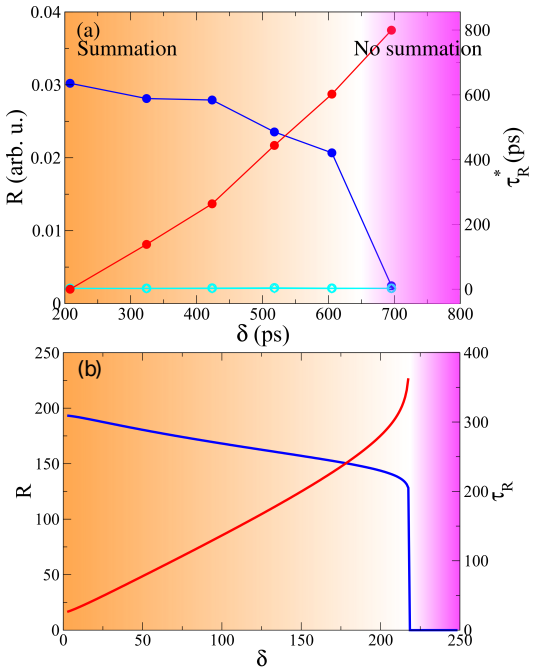

Figure 4. (a)Median of the maximum response R (blue) from experimental data in Fig.2 for two consecutive stimuli separated by the delay δ. The response to each perturbation alone is plotted in light blue (empty diamond, empty circle respectively). The response delay (relative to the shortest response delay) τ^*_R is shown in red. (b) Same for model with parameters : $\mu = 2.48$, $\mu_1 = 0.43$, $\mu_2 = 0.43$, $s = 10$, $\gamma_g = 0.005$, $\gamma_{as} = 0.01$, $\gamma = 2$, $\eta = 1.6$, $\beta = 1 \times 10^{-5}$. The response delay τ_R is relative to the second perturbation.

saturation parameter, γ the linear losses and β the spontaneous emission factor. The term $G + \eta$ is directly proportional to the carrier density in the gain section. The β parameter is small here and steady state solutions can be expended in power series of β [12]. Let $\{I_{ss}, G_{ss}, Q_{ss}\}$ be a steady state solution of Eqs.3. A simple approach to get an analytic insight into the dynamics is to consider that the intensity is small ($I_{ss} \propto \beta$) and almost constant as long as a pulse has not been triggered. Suppose at time $t = 0$ a first delta-like sub-threshold perturbation is sent e.g. on the gain followed by a second perturbation on at time $t = \delta$ (in units of the photon lifetime in the cavity) such that $\mu \to \mu + \mu_1 \delta_D(t) + \mu_2 \delta_D(t - \delta)$, where δ_D is the Dirac delta function. We can then solve for $G(t)$ such that

$$G(t) = G_{ss} + \Pi(t)\mu_1 \exp\left[\frac{-\gamma_g t}{1 + I_{ss}}\right] + \Pi(t-\delta)\mu_2 \exp\left[\frac{-\gamma_g (t-\delta)}{1 + I_{ss}}\right] \quad (4)$$

with $\Pi(t)$ the unit-step function. As noted in [12], in a first approximation the net gain $R(t) = G(t) - Q(t) - 1$ governs the triggering of an excitable pulse : a pulse can only be excited if $R(t)$ exceeds zero for a sufficiently large amount of time. Hence the final state of the system is controlled by the net gain immediately after the second perturbation at $t = \delta^+$ (always considering a first, sub-threshold stimulus). Numerical simulations are shown on Fig.5. The net gain is plotted together with the response to the consecutive stimuli. Simulations of the full system (Eqs.3) and of the approximate solution (Eqs.4) for the net-gain are shown. The parameters are similar to the one used in [12] except the recombinations rates that have been tuned to match better the experimental results. With the estimated photon lifetime of the empty cavity being 3.25ps, a reasonable qualitative agreement is met between the model and the experiment. The critical delay is found to be $\delta_c \simeq 218$, that is to say 708ps in physical units with the estimated photon lifetime. This is in reasonable agreement with the experimental value in Fig.4a between 600 and 700ps and for incoherent perturbation conditions similar to those of the experiment: namely, consecutive perturbations of amplitude 74% of the single perturbation excitable threshold μ_{ex} with the pump at 91% of the self-pulsing threshold (corresponding here to the numerical value of 2.88). The sub-threshold dynamics of the net gain is very well reproduced by the linear approximation solution until it completely fails when a pulse is triggered, as expected. For the longest delay ($\delta = 244$), when the summed perturbations are sub-threshold, the approximate net gain deviates from the full solution after the second perturba-

tion because it passes close to 0 and hence the intensity dynamics, even failing to trigger an excitable response, has a non-negligible influence on it. The response and the delay in the response versus delay between the sub-threshold stimuli are shown in Fig.4b. A good agreement is found with the experimental results. The response abruptly switches to zero when the delay δ is larger than a critical delay $\delta_c \simeq 218$. At this point, the response delay τ_R diverges as one expects. Note that there is a point for the response delay τ_R in the experimental curve (Fig.4) even after the critical delay δ_c because of noise that is able to trigger a few excitable pulses even for stimuli on average below the excitable threshold. These events are taken into account for the determination of τ_R. The divergence of the delay for perturbations close to the excitable threshold is also responsible for the large dispersion in response times clearly visible in Fig.2d-f) because a larger number of stimuli will be brought just above the excitable threshold in these cases. It is interesting to notice that the final state of the system is different for asymmetric perturbations: for a balanced perturbation such that $\mu_1 + \mu_2$ is constant, the highest net gain at time δ is obtained for asymmetric perturbations with $\mu_1 < \mu_2$. This slight effect means that the temporal summation considered here is a non-commutative operation.

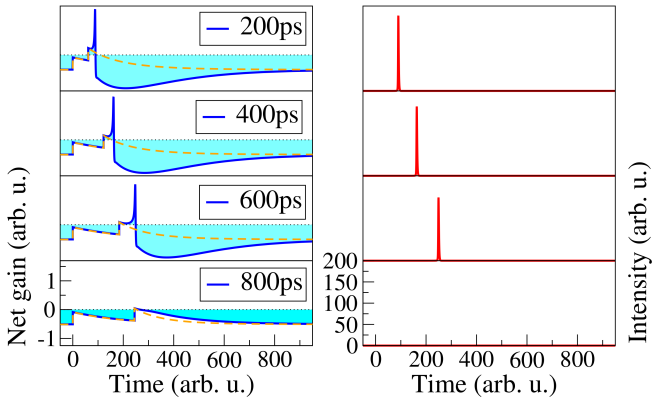

Figure 5. Numerical simulations of the system Eqs.3 showing the response to two sub-threshold stimuli on the gain ($\mu_{1,2}$) with a variable delay δ : net gain (blue), intensity (red) and linear solution (Eqs4, orange dashed line). Parameters are the same as in Fig.4. The excitable threshold is $\mu_{ex} \simeq 0.581$, and $\mu_1 = \mu_2 = 0.74\mu_{ex}$. The delays are $\delta = 61,\ 122,\ 183$ and 244 corresponding respectively to physical delays of 200, 400, 600 and 800ps.

The critical delay is computed for two input stimuli of equal amplitudes μ_0 in Fig.6. For an amplitude $\mu_0 < 0.37$, temporal summation never occurs since the summed stimuli are not large enough to cross the excitable threshold even for zero delay. On the contrary, for larger stimuli the maximum possible delay giving rise to an excitable response increases first almost linearly with the stimulus strength. When a single stimulus is almost able to trigger an excitable response obviously the maximum delay increases and diverges.

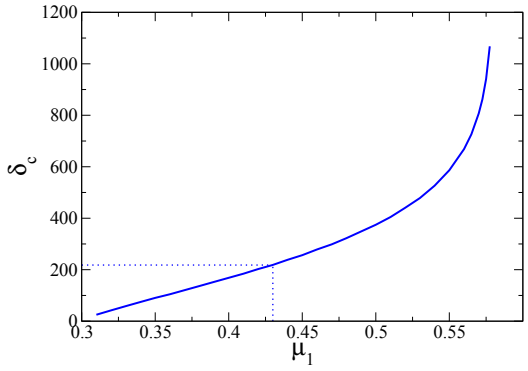

Figure 6. Critical delay δ_c versus amplitude of the two stimuli for $\mu_1 = \mu_2$. Dashed lines correspond to the case of Fig.4(b) and $\mu_1 = \mu_2 = 0.43$.

In conclusion we have studied the effect of consecutive sub-threshold stimuli on the response of a semiconductor micropillar neuromimetic system. We have shown that the system can integrate stimuli with a time constant of the order of several hundreds of picoseconds which depends on the recombination times of carriers in the active medium and respond with a macroscopic, excitable pulse if the time delay between the stimuli is shorter than a critical delay. The critical delay depends on the excitable threshold which is controllable by the amount of pumping of the system. This system thus simulates the behavior of a leaky integrate-and-fire neuron and is particularity suited for building more advanced processing functionalities. Incoherent and coherent perturbation schemes have been demonstrated, the latter being important to demonstrate cascadability of such excitable systems. As was demonstrated in [23], a sufficient number of excitable processing units coupled appropriately is capable of universal computation. It is however important to keep in mind that even a single unit has also processing capabilities [3]. In the case of two stimuli, this system behaves as a fast optical coincidence detector, a functionality that may be of importance in many applications like pattern recognition in optical signals, in analogy to biological systems using these property for sound localization [20].

FUNDING INFORMATION

This work was partially supported by the French Renatech network for the nanofabrication of the samples.

* sylvain.barbay@lpn.cnrs.fr

[1] D. Woods and T. J. Naughton, Nat Phys **8**, 257 (2012).

[2] A. N. Tait, M. A. Nahmias, Y. Tian, B. J. Shastri, and P. R. Prucnal, in "Nanophotonic Information Physics," , M. Naruse, ed., pp. 183 (Springer, 2014).
[3] C. Koch and I. Segev, Nature Neuroscience **3**, 1171 (2000).
[4] M. Giudici, C. Green, G. Giacomelli, U. Nespolo, and J. R. Tredicce, Phys. Rev. E **55**, 6414 (1997).
[5] H. J. Wünsche, O. Brox, M. Radziunas, and F. Henneberger, Phys. Rev. Lett. **88**, 023901 (2001).
[6] S. Barland, O. Piro, M. Giudici, J. R. Tredicce, and S. Balle, Phys. Rev. E **68**, 036209 (2003).
[7] A. M. Yacomotti, P. Monnier, F. Raineri, B. B. Bakir, C. Seassal, R. Raj, and J. A. Levenson, Phys. Rev. Lett. **97**, 143904 (2006).
[8] D. Goulding, S. P. Hegarty, O. Rasskazov, S. Melnik, M. Hartnett, G. Greene, J. G. McInerney, D. Rachinskii, and G. Huyet, Phys. Rev. Lett. **98**, 153903 (2007).
[9] S. Beri, L. Mashall, L. Gelens, G. V. der Sande, G. Mezosi, M. Sorel, J. Danckaert, and G. Verschaffelt, Phys. Lett. A **374**, 739 (2010).
[10] T. V. Vaerenbergh, M. Fiers, P. Mechet, T. Spuesens, R. Kumar, G. Morthier, B. Schrauwen, J. Dambre, and P. Bienstman, Opt. Express **20**, 20292 (2012).
[11] S. Barbay, R. Kuszelewicz, and A. M. Yacomotti, Opt. Lett. **36**, 4476 (2011).
[12] F. Selmi, R. Braive, G. Beaudoin, I. Sagnes, R. Kuszelewicz, and S. Barbay, Phys. Rev. Lett. **112**, 183902 (2014).
[13] E. M. Izhikevich, Neural Networks **14**, 883 (2001).
[14] K. Alexander, T. V. Vaerenbergh, M. Fiers, P. Mechet, J. Dambre, and P. Bienstman, Opt. Express **21**, 26182 (2013).
[15] B. Garbin, J. Javaloyes, G. Tissoni, and S. Barland, Nat Commun **6**, 5915 (2015).
[16] M. Nahmias, B. Shastri, A. Tait, and P. Prucnal, IEEE J. Sel. Topics Quantum Electron. **19**, 1 (2013).
[17] E. Izhikevich, IEEE Trans. Neural Netw. **15**, 1063–1070 (2004).
[18] K. S. Kravtsov, M. P. Fok, P. R. Prucnal, and D. Rosenbluth, Opt. Express **19**, 2133 (2011).
[19] B. J. Shastri, A. N. Tait, M. Nahmias, B. Wu, and P. Prucnal, in "CLEO: 2014," (Optical Society of America, 2014), p. STu3I.5.
[20] J. L. Peña and W. M. DeBello, ILAR journal **51**, 338 (2010).
[21] T. Elsass, K. Gauthron, G. Beaudoin, I. Sagnes, R. Kuszelewicz, and S. Barbay, Eur. Phys. J. D **59**, 91 (2010).
[22] J. L. A. Dubbeldam, B. Krauskopf, and D. Lenstra, Phys. Rev. E **60**, 6580 (1999).
[23] W. S. McCulloch and W. Pitts, The bulletin of mathematical biophysics **5**, 115 (1943).